Available online at www.sciencedirect.com
ScienceDirect
Journal of Sound and Vibration 313 (2008) 77–96
JOURNAL OF SOUND AND VIBRATION
www.elsevier.com/locate/jsvi

Thermoelastic damping in the contour-mode vibrations of micro- and nano-electromechanical circular thin-plate resonators

Zhili Hao*

Department of Mechanical Engineering, Old Dominion University, 238 Kaufman Hall, Norfolk, VA 23529-0247, USA

Received 18 April 2007; received in revised form 6 November 2007; accepted 19 November 2007
Available online 27 February 2008

Abstract

This paper presents an analytical study on thermoelastic damping (TED) in the contour-mode vibrations of micro- and nano-electromechanical circular thin-plate resonators. Instead of expressing TED in terms of a commonly used complex frequency value, this work calculates TED by using a thermal-energy approach in which the generation of thermal energy per cycle of vibration is considered. To demonstrate its validity, this thermal-energy approach is first utilized to tackle the well-known TED in a flexural-mode beam resonator. Then, it is extended to analyzing TED in the contour-mode vibrations of a circular thin-plate micro-/nano-resonator. Consequently, the behavior of TED versus the key design parameters, namely thin-plate radius and resonant frequency, is predicted, and the attainable quality factors of such type of resonators are defined. From this work, it is found that the Q_{TED} of the contour-mode vibrations of a circular thin-plate resonator is well above 1×10^6 when its resonant frequency is below 1 GHz and TED becomes a significant source of dissipation for circular thin-plate resonators at the nanometer scale.

1. Introduction

Micro- and nano-electromechanical (MEM/NEM) resonators are of great interests for a wide range of sensing [1–3] and electrical filtering [4–7] applications. For these applications, it is important to design and fabricate resonators with very high-quality factors or very little energy dissipation. Owing to its small size, it is feasible to package a MEM and NEM resonator in vacuum and thereby eliminate air damping. Consequently, other dissipation mechanisms [8–11], such as thermoelastic damping (TED), support loss, and surface loss, now come to the fore and become the major bottlenecks for these resonators' performance. Among the dissipation mechanisms, TED imposes an upper limit on the attainable quality factor of a MEM and NEM resonator. It is therefore desirable to accurately predict TED, not only for improving the performance of these resonators but also for establishing their performance limits.

*Tel.: +1 757 683 6734; fax: +1 757 683 5344.
E-mail address: zlhao@odu.edu

0022-460X/$ - see front matter © 2007 Elsevier Ltd. All rights reserved.
doi:10.1016/j.jsv.2007.11.035

Nomenclature

A	cross-section area of a beam (μm^2)
b	beam width (μm)
C_p	specific heat (J/kg K)
E	Young's modulus (GPa)
h	beam and thin-plate thickness (μm)
I	moment of inertia (μm^4)
k	frequency parameter of the contour-mode vibrations
k_b, ξ_b	variables related to thermoelastic damping in a beam resonator
k_p, ξ_p	variables related to thermoelastic damping in a circular thin-plate resonator
L	beam length (μm)
m	contour-mode order
Q	quality factor
ΔQ	generation of thermal energy per cycle of vibration (J)
r	radial variable (μm)
r'	normalized radial variable
R	radius of a thin-plate (μm)
s	entropy (J/K)
t_0	time period of vibration (s)
T_0	initial temperature (K)
W	maximum stored vibration energy (J)
ΔW	energy dissipated per cycle of vibration (J)
$\vec{u}$	elastic displacement vector (μm)
u_r	radial displacement (μm)
u_θ	circumferential displacement (μm)
$\nabla \cdot \vec{u}$	elastic dilatation
U_b	vibration amplitude of a beam (μm)
U_p/R	vibration amplitude of a thin-plate (μm)
y	y-axis variable
y'	normalized y-axis variable
Y_0	uncoupled flexural-mode vibration shape
α_T	linear thermal expansion coefficient (K^{-1})
β_{T2D}	coefficient for thermal expansion in 2D cases (Pa/K)
β_{T3D}	coefficient for thermal expansion in 3D cases (Pa/K)
γ_b	mode shape factor of a beam resonator
γ_p	mode shape factor of a circular thin-plate resonator
Δ_E	thermal relaxation strength
θ	circumferential variable (rad)
Θ	temperature variation (K)
Θ_s	general solution to the temperature variation in a circular thin-plate resonator (K)
Θ_T	particular solution to the temperature variation in a circular thin-plate resonator (K)
κ	thermal conductivity (W/m K)
λ_{2D}	Lame coefficient in 2D cases (GPa)
λ_{3D}	Lame coefficient in 3D cases (GPa)
μ_{2D}	Lame coefficient in 2D cases (GPa)
μ_{3D}	Lame coefficient in 3D cases (GPa)
Π	variable for the temperature variation
Π_1	integral constant related to the general solution of the temperature variation
Π_2	integral constant related to the particular solution of the temperature variation
ρ	density (kg/m^3)
Σ	integral constant for the contour mode
υ	Poisson's ratio
χ	thermal diffusivity (m^2/s)
ω	angular resonant frequency (rad/s)

With the increasing demand of MEM and NEM resonators with very high frequencies and very high-quality factors, free-edged circular thin-plate resonators operating in their contour-modes have attracted great attention [12–14], because this type of resonators can achieve high resonant frequencies without the need to scale the resonator dimensions into the nanometer domain, therefore easing fabrication and reducing surface loss. Furthermore, by locating a small support beam at the resonant node of a circular thin-plate resonator, support loss in the resonator is substantially alleviated [12,13,15]. It is well known that TED is significant at low frequencies of the flexural-mode vibrations of a beam resonator, while it becomes noticeable at extremely high frequencies of the longitudinal-mode vibrations of a beam (also referred to as block) resonator. Now, the question arises: how TED behaves in the contour-mode vibrations of a circular thin-plate resonator? This work addresses this question through utilizing a thermal-energy approach, in which the generation of thermal energy per cycle of vibration is considered.

This paper is organized as follows. The following section presents the governing equations of linear thermoelasticity in general. Section 3 presents an overview of two approaches for calculating TED: complex frequency and thermal energy. Since the thermal-energy approach has not been utilized for analyzing TED in a mechanical resonator yet, Section 4 is dedicated to demonstrating its validity with the well-known solution

to TED in a flexural-mode beam resonator. In Section 5, this thermal-energy approach is extended to analyzing TED in the contour-mode vibrations of a free-edged circular thin-plate resonator. The significant insights of this work are discussed and concluded at the end.

2. Governing equations of linear thermoelasticity

The laws of thermodynamics predict that variation of strain in a solid is accompanied by a variation of temperature, which causes an irreversible flow of heat. This heat conduction gives rise to an increase in entropy, or the generation of thermal energy, and consequently, to dissipation of vibration energy. This process of energy dissipation is commonly referred to as TED.

Consider a homogenous and isotropic solid medium that is initially at a uniform temperature T_0. In the absence of internal heat source and body force, the governing equations of linear thermoelasticity are written as [16]

$$(\lambda + 2\cdot\mu)\cdot\nabla(\nabla\cdot\vec{u}) - \mu\cdot\nabla\times\nabla\times\vec{u} - \beta_T\cdot\nabla\Theta = \rho\cdot\frac{\partial^2\vec{u}}{\partial t^2} \tag{1a}$$

and

$$\kappa\cdot\nabla^2\Theta - C_p\cdot\rho\cdot\frac{\partial\Theta}{\partial t} = \beta_T\cdot T_0\cdot\frac{\partial}{\partial t}(\nabla\cdot\vec{u}), \tag{1b}$$

where κ, ρ, and C_P are the thermal conductivity, density, and specific heat of the solid medium, respectively. While λ and μ are Lame coefficients, β_T is a coefficient related to thermal expansion effect of the solid medium. In terms of the material properties, these coefficients can be expressed in three-dimensional (3D) cases and two-dimensional (2D) cases, respectively, as below [16]:

$$\lambda_{3D} = \frac{\upsilon E}{(1+\upsilon)(1-2\upsilon)}, \quad \mu_{3D} = \frac{E}{2(1+\upsilon)} \quad \text{and} \quad \beta_{T3D} = \frac{\alpha_T E}{1-2\upsilon} \tag{2a}$$

$$\lambda_{2D} = \frac{\upsilon E}{1-\upsilon^2}, \quad \mu_{2D} = \frac{E}{2(1+\upsilon)} \quad \text{and} \quad \beta_{T2D} = \frac{\alpha_T E}{1-\upsilon}, \tag{2b}$$

where E, υ, and α_T are the Young's modulus, Poisson's ratio, and linear thermal expansion coefficient of the solid medium, respectively.

In the above two thermoelastic-coupled governing equations, $\vec{u}$ and $\Theta = T - T_0$ denote the elastic displacement vector and the temperature variation from the initial temperature T_0, respectively. While the last term on the left-hand side of the elastic equation (1a) represents the stress caused by the temperature variation in the solid medium, the term on the right-hand side of the heat conduction equation (1b) represents the temperature variation resulted from the elastic dilatation, which is expressed as $\nabla\cdot\vec{u}$, in the solid medium. These two terms are the factors coupling the elastic vibrations and the temperature variation together.

3. Two approaches for calculating TED

Calculating TED is a well-defined problem—solve the two coupled equations for the dissipation of vibration energy per cycle of vibration. Although the physical mechanism and theory of thermoelasticity have been well established [16], there are very few analytical solutions to TED in the vibrations of finite geometries, due to the complexity in mathematical derivation [17]. In the 1930s, Zener [18,19] derived an approximate solution to TED in flexural-mode beam resonators. His theory showed that TED in a beam exhibits a Lorentzian behavior with a single thermal relaxation time. A few years ago, Lifshitz and Roukes [9] provided an exact solution to TED in micro- and nano-mechanical beam resonators, predicting a modified Lorentzian behavior of TED. Recently, TED in ring resonators was also addressed [20,21].

All the aforementioned works are based on the fundamental assumption that thermoelastic coupling is very weak and has negligible influence on the uncoupled elastic vibration modes of a mechanical resonator, so the

elastic and thermal problems are essentially decoupled. Following this assumption, the uncoupled elastic vibration modes from the elastic equation are further assumed and their corresponding elastic dilatation is derived. Then, the substitution of the elastic dilatation into the heat conduction equation leads to the expression for the temperature variation in the resonator. Here, it should be noted that both the elastic vibrations and the temperature variation are assumed to be time harmonic with the same resonant frequency. Upon knowing both the elastic dilatation, $\nabla \cdot \vec{u}$, and the temperature variation, Θ, two approaches can be utilized for calculating TED, as described below.

3.1. Complex-frequency approach

In the complex-frequency approach, the effect of TED on the elastic vibrations of a mechanical resonator is taken into account by expressing the resonant frequency as a complex value:

$$\omega = (\omega_r + \omega_i \mathrm{i}) \quad \text{with} \quad \omega_r, \quad \omega_i \geqslant 0 \quad \text{and} \quad \mathrm{i} = \sqrt{-1}, \tag{3}$$

where ω_r is the real value giving the new resonant frequency of the mechanical resonator in the presence of thermoelastic coupling, while ω_i is the imaginary value giving the calculation of TED. To obtain the expression for the complex frequency, the temperature variation is substituted into the coupled elastic equation (1a) and gives rise to a complex Young's modulus. Incorporating the complex Young's modulus into the equation for the resonant frequency leads to an explicit expression for the complex frequency. Consequently, in terms of the derived complex frequency, the quality factor related to TED, Q_{TED}, can be calculated as [9]

$$Q_{\mathrm{TED}}^{-1} = 2\left|\frac{\mathrm{Im}(\omega)}{\mathrm{Re}(\omega)}\right|. \tag{4}$$

By utilizing this complex-frequency approach, the solutions to TED in both beam [9] and ring [20,21] resonators have been obtained. The details about this approach can be found in the related works [9,20,21] and therefore are not elaborated here. However, it should be noted that this approach requires substituting the temperature variation into the coupled elastic equation (1a), in order to obtain a complex Young's modulus. This makes it extremely difficult, if not impossible, to solve TED in complex cases, such as the contour-mode vibrations of a circular thin-plate resonator.

3.2. Thermal-energy approach

In fact, besides interpreted as the dissipation of vibration energy, TED can also be interpreted as the generation of thermal energy per cycle of vibration, which is the very essence of TED [19]. Therefore, one may calculate TED by seeking this generation of thermal energy per cycle of vibration. Now, we describe the procedure of deriving the expression for the generation of thermal energy, in terms of the known elastic dilatation and temperature variation. It should be emphasized that, in this thermal-energy approach, the resonant frequency holds a real value and thus is different from that used in the complex-frequency approach. For simplicity, the elastic dilatation is assumed to have a real value. Then, the temperature variation must become complex because of thermoelastic coupling.

Owing to heat conduction, the entropy of an infinitesimal element volume in a mechanical resonator, $\mathrm{d}v$, changes at a rate of [19]

$$\frac{\mathrm{d}s}{\mathrm{d}t} = \frac{\kappa \cdot \nabla^2 T}{T}\,\mathrm{d}v, \tag{5}$$

where s is the entropy of the element. The temperature can be represented by $T = T_0 + \Theta$, where the relation $\Theta \ll T_0$ exists, because the temperature variation due to thermoelastic coupling is very small. By using Taylor-series expansion and neglecting the higher-order expansion terms, Eq. (5) can be rewritten as

$$\frac{\mathrm{d}s}{\mathrm{d}t} = \left(1 - \frac{\Theta}{T_0}\right)\frac{\kappa \cdot \nabla^2 \Theta}{T_0}\,\mathrm{d}v. \tag{6}$$

Then, substituting Eq. (1b) into Eq. (6) leads to the following relation:

$$\frac{\mathrm{d}s}{\mathrm{d}t} = \left(1 - \frac{\Theta}{T_0}\right)\frac{\rho C_P}{T_0}\left[\frac{\partial\Theta}{\partial t} + \frac{\beta_T T_0}{\rho C_p}\frac{\partial}{\partial t}(\nabla\cdot\vec{u})\right]\mathrm{d}v. \tag{7}$$

According to the definition of entropy [22], the thermal energy generated by irreversible heat conduction is written as

$$\mathrm{d}Q = T_0\,\mathrm{d}s, \tag{8}$$

where the relation $\Theta \ll T_0$ has been applied. Substituting Eq. (7) into Eq. (8) and integrating the later equation over one time period of vibration, t_0, and across the whole volume of a mechanical resonator gives rise to the expression for the generation of thermal energy per cycle of vibration:

$$\Delta Q = \rho C_P \int_0^{t_0}\int_0^{V}\left(1 - \frac{\Theta}{T_0}\right)\left[\frac{\partial\Theta}{\partial t} + \frac{\beta_T T_0}{\rho C_p}\frac{\partial}{\partial t}(\nabla\cdot\vec{u})\right]\mathrm{d}v\,\mathrm{d}t. \tag{9}$$

As mentioned previously, both the elastic dilatation and the temperature variation are time harmonic with the same real resonant frequency, $\sim e^{i\omega t}$, but the elastic dilatation has a real value and the temperature variation is complex. For this reason, Eq. (9) can be rewritten as

$$\Delta Q = -\beta_T \int_0^{t_0}\int_0^{V}\Theta\frac{\partial}{\partial t}(\nabla\cdot\vec{u})\,\mathrm{d}v\,\mathrm{d}t. \tag{10}$$

The integral in Eq. (10) can easily be solved in mathematical software, such as Matlab. The real part of the above expression, $\mathrm{Re}(\Delta Q)$, is equal to the generation of thermal energy per cycle of vibration, or thermoelasic damping, ΔW. In turn, this suggests that the imaginary part of the temperature variation is out of phase with the elastic dilatation and contributes to TED, since the derivative of the elastic dilatation ($\sim e^{i\omega t}$) with respect to time is a pure imaginary value.

Based on the definition of the mechanical quality factor [23]

$$Q = 2\pi\frac{W}{\Delta W}, \tag{11}$$

where ΔW denotes the energy dissipated per cycle of vibration and W denotes the stored maximum vibration energy in a mechanical resonator, substituting the real part of Eq. (10) into Eq. (11) gives rise to the calculation of Q_{TED}. To the author's knowledge, this thermal-energy approach has so far not been utilized for analyzing TED in a mechanical resonator. Therefore, Section 4 is dedicated to demonstrating its validity with the well-known solution to TED in a flexural-mode beam resonator.

4. TED in the flexural-mode vibrations of a beam resonator

In Section 4, we briefly review uncoupled elastic vibrations and heat conduction in a flexural-mode beam resonator and describe how the elastic dilatation and the temperature variation can be combined to obtain the solution to TED.

4.1. Elastic dilatation in the uncoupled elastic vibrations

Fig. 1 shows a schematic view of a beam resonator. The length, width, and thickness of the beam are denoted by L, b, and h, respectively. For simplicity, it is assumed that the ratio of the beam length to the beam width is larger than 20 ($L/b > 20$), so that the Euler–Bernoulli beam theory can be used for the related vibration analysis [24]. Being clamped at one end or at both ends, this beam vibrates in its x–y plane flexural mode, and the governing equation for its elastic vibrations is written as [8]

$$\frac{\partial^4 Y}{\partial x^4} = -\frac{\rho A}{EI}\frac{\partial^2 Y}{\partial t^2}, \tag{12}$$

where $I = b^3h/12$ and $A = bh$ are the moment of inertia and the cross-section area of the beam, respectively.

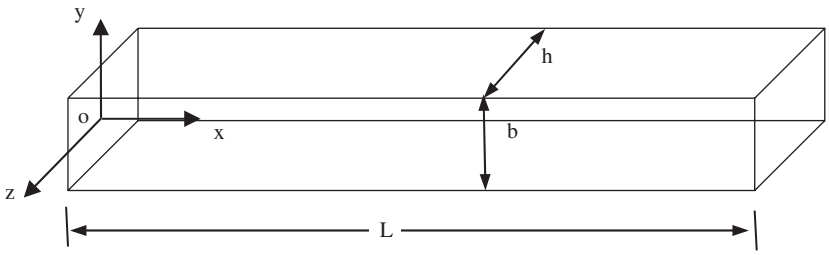

Fig. 1. Schematic view of a beam resonator and its associated coordinates.

The beam resonator undergoes time-harmonic vibrations, $Y_0 \ldots e^{j\omega t}$, with the resonant frequency, ω, expressed as below:

$$\omega = \frac{\pi^2\beta^2}{L^2}\sqrt{\frac{EI}{\rho A}}, \tag{13}$$

where β denotes the mode constant. The uncoupled flexural-mode vibration shape is expressed as [8]

$$Y_0 = \frac{U_b}{2}\left\{\cosh\left(\beta\pi\frac{x}{L}\right) - \cos\left(\beta\pi\frac{x}{L}\right) + \gamma_b\left(\sinh\left(\beta\pi\frac{x}{L}\right) - \sin\left(\beta\pi\frac{x}{L}\right)\right)\right\}, \tag{14}$$

where constants γ_b and U_b denote the made shape factor and the vibration amplitude, respectively. The stored maximum vibration energy in the beam resonator is calculated as [8]

$$W = \tfrac{1}{8}\rho AL\omega^2 U_b^2. \tag{15}$$

The elastic dilation due to the uncoupled flexural-mode elastic vibrations and the temperature variation is expressed as [9]

$$\nabla\cdot\vec{u} = (2\upsilon - 1)y\frac{d^2Y_0}{dx^2}e^{i\omega t} + 2(1+\upsilon)\alpha_T\Theta. \tag{16}$$

Compared with its first term, the second term of the elastic dilatation in Eq. (16) has negligible effect on heat conduction [9] and therefore will be omitted in the following heat conduction analysis.

4.2. Temperature variation due to the elastic dilatation

Owing to the high ratio of the beam length to the beam width ($L/b > 20$), the temperature gradient along the beam length is much smaller than that across the beam width. Thus, heat conduction in the beam is assumed to occur only along the y-axis direction. Accordingly, the heat conduction equation (1b) can be simplified as

$$\chi\frac{\partial^2\Theta}{\partial y^2} - \frac{\partial\Theta}{\partial t} = \frac{\beta_{T3D}T_0}{\rho C_P}\frac{\partial}{\partial t}(\nabla\cdot\vec{u}). \tag{17}$$

The temperature variation is assumed to be time harmonic with the same frequency as the elastic vibrations, $\Theta = \Theta_0(x)e^{i\omega t}$. With the aid of Eq. (16), Eq. (17) can be rewritten as

$$\frac{\partial^2\Theta_0}{\partial y^2} + \frac{\omega}{i\chi}\Theta_0 = \frac{\omega}{i\chi}\frac{\Delta_E}{\alpha_T}y\frac{d^2Y_0}{dx^2}, \tag{18}$$

where $\Delta_E = E\alpha_T^2T_0/\rho C_p$ is the thermal relaxation strength that is related to the material properties and the initial temperature. The solution to Eq. (18) can be written as below:

$$\Theta_0 = B_1\sin(k_by) + B_2\cos(k_by) + \frac{\Delta_E}{\alpha_T}y\frac{d^2Y_0}{dx^2}, \tag{19}$$

where B_1 and B_2 are two constants; and

$$k_b = \sqrt{\frac{\omega}{\mathrm{i}\chi}} = (1-\mathrm{i})\frac{\xi_b}{b} \quad \text{with} \quad \xi_b = b\sqrt{\frac{\omega}{2\chi}} \quad \text{and} \quad \mathrm{i} = \sqrt{-1}. \tag{20}$$

Applying the adiabatic boundary condition at the boundaries of $y = \pm b/2$ to Eq. (19) leads to the explicit expression for the temperature variation across the beam width:

$$\Theta_0 = \frac{\Delta_E}{\alpha_T}\frac{\mathrm{d}^2 Y_0}{\mathrm{d}x^2} b\left[\frac{y}{b} - \frac{\sin(k_b y)}{k_b b\cos(k_b b/2)}\right]. \tag{21}$$

Because of the complex expression for k_b in Eq. (20), the temperature variation in Eq. (21) is complex. While its real part is in phase with the elastic vibrations, the imaginary part of the temperature variation is out of phase with the elastic vibrations and causes TED. Furthermore, the first term of the temperature variation is the particular solution corresponding to the elastic dilatation and its second term is the general solution resulting from heat conduction. The temperature variation from the elastic dilatation holds a real value and therefore does not contribute to TED. In contrast, the temperature variation from the general solution is complex, indicating that part of its heat conduction is irreversible and causes TED. Fig. 2 illustrates the behavior of the real and imaginary parts of the general solution and the particular solution as functions of the beam width, b, and the variable, ξ_b.

4.3. Solution to TED

The elastic dilatation, Eq. (16), and the temperature variation, Eq. (21), are substituted into Eq. (10), giving rise to the following expression:

$$\Delta Q = -\frac{\kappa}{T_0\chi}\left(\frac{\Delta_E}{\alpha_T}\right)^2 \pi \mathrm{i} IL\left(\frac{\beta\pi}{L}\right)^4\left(\frac{U_b}{2}\right)^2\left[1 - \frac{24}{b^3 k_b^3}(\tan(k_b b/2) - k_b b/2)\right], \tag{22}$$

where

$$1 - \frac{24}{(k_b b)^3}(\tan(k_b b/2) - k_b b/2) = 1 - \frac{6}{\xi_b^3}\frac{\sinh(\xi_b) - \sin(\xi_b)}{\cos(\xi_b) + \cosh(\xi_b)} - \frac{6}{\xi_b^3}\left[\xi_b - \frac{\sin(\xi_b) + \sinh(\xi_b)}{\cos(\xi_b) + \cosh(\xi_b)}\right]\mathrm{i}. \tag{23}$$

Corresponding to the imaginary part of the temperature variation, the real part of Eq. (22) is equal to the generation of thermal energy per cycle of vibration:

$$\mathrm{Re}(\Delta Q) = \frac{\kappa}{T_0\chi}\left(\frac{\Delta_E}{\alpha_T}\right)^2 \pi IL\left(\frac{\beta\pi}{L}\right)^4\left(\frac{U_b}{2}\right)^2 \frac{6}{\xi_b^3}\left[\xi_b - \frac{\sinh(\xi_b) + \sin(\xi_b)}{\cosh(\xi_b) + \cos(\xi_b)}\right]. \tag{24}$$

The combination of Eqs. (11), (15), and (24) leads to the explicit expression for the Q_{TED} of the flexural-mode vibrations of a rectangular beam resonator:

$$Q_{\mathrm{TED}}^{-1} = \Delta_E\left[\frac{6}{\xi_b^2} - \frac{6}{\xi_b^3}\frac{\sinh(\xi_b) + \sin(\xi_b)}{\cosh(\xi_b) + \cos(\xi_b)}\right]. \tag{25}$$

This solution to TED in a flexural-mode beam resonator is exactly the same as that obtained through the complex-frequency approach [9]. Therefore, the validity of the thermal-energy approach is demonstrated.

5. TED in the contour-mode vibrations of a circular thin-plate resonator

Section 5 focuses upon solving TED in the contour-mode vibrations of a circular thin-plate resonator by using the above verified thermal-energy approach. Fig. 3 illustrates a schematic view of a circular thin-plate resonator with its polar coordinates (r, θ) originated at the center of the thin plate. This resonator has a radius of R and is initially at a uniform temperature T_0. It is assumed that the circular thin-plate resonator is free edged [12], homogeneous, isotropic, and in the case of 2D plane stress; and thus the elastic vibrations and the temperature variation are independent of its thickness, h.

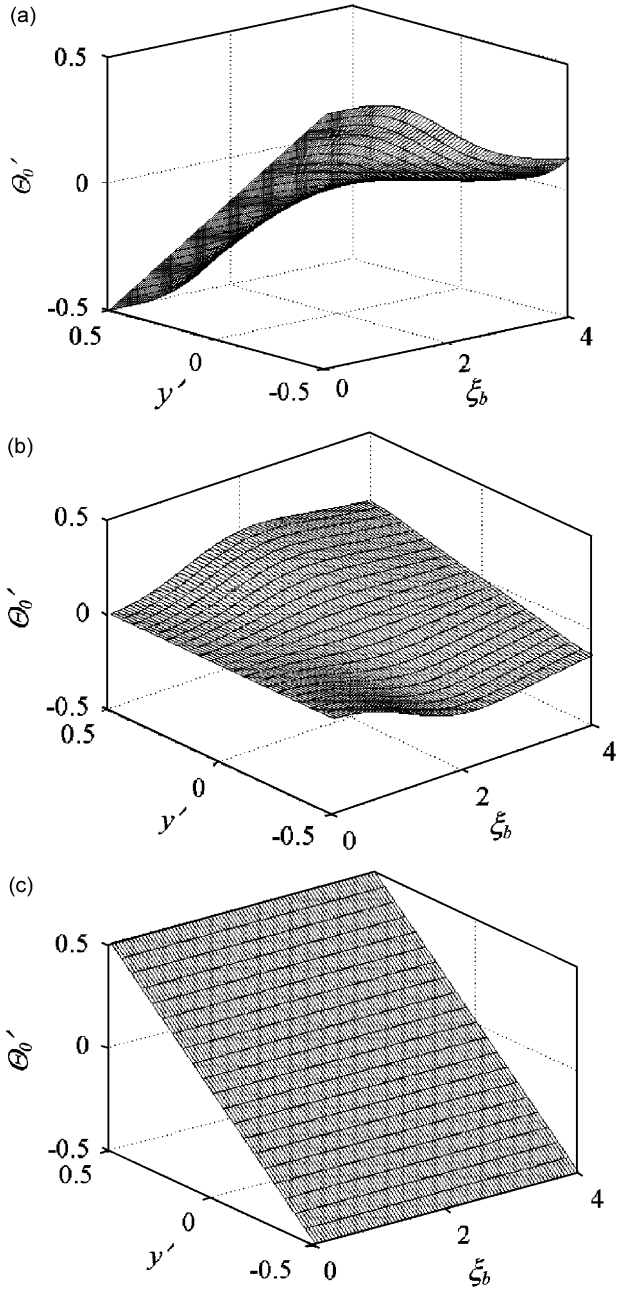

Fig. 2. The behavior of the temperature variation across the beam width at different values of the variable, ξ_b: (a) real part of the general solution, (b) imaginary part of the general solution, and (c) particular solution. *Note*: y is normalized to the beam width: $y' = y/b$, $\xi_b \in (0.1, 4)$, and $\Theta_0' = \Theta_0/((\Delta_E/\alpha_T)(\mathrm{d}^2 Y/\mathrm{d}x^2)b)$.

5.1. Elastic dilatation in the uncoupled contour-mode elastic vibrations

According to Eq. (1a), in the absence of thermoelastic coupling, the governing equations for the contour-mode vibrations in a circular thin-plate resonator are written as [12]

$$\left(\lambda_{2D} + 2\mu_{2D}\right) \cdot \nabla(\nabla \cdot \vec{u}) - \mu_{2D} \cdot \nabla \times \nabla \times \vec{u} = \rho \cdot \frac{\partial^2 \vec{u}}{\partial t^2}, \tag{26}$$

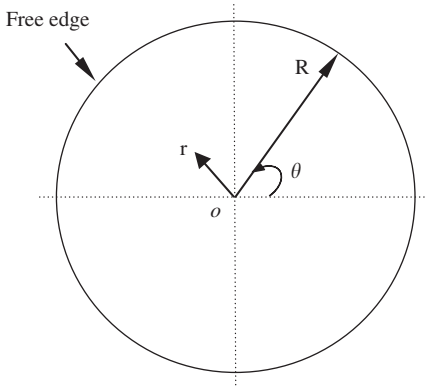

Fig. 3. Schematic view of a free-edged circular thin-plate resonator with the thickness, h.

where the displacement vector $\vec{u}$ is defined in terms of the radial displacement, u_r, and circumferential displacement, u_θ, respectively, expressed as below:

$$\vec{u} = u_r \cdot \vec{r} + u_\theta \cdot \vec{\theta}. \tag{27}$$

When this resonator goes through time-harmonic vibrations, we can assume

$$u_r = u_{r0} e^{i\omega t} \quad \text{and} \quad u_\theta = u_{\theta 0} e^{i\omega t}, \tag{28}$$

where ω denotes the resonant frequency of the contour-mode vibrations. The resonant frequency of the mth order contour-mode vibrations is expressed as

$$\omega = \frac{k}{R}\sqrt{\frac{E}{\rho(1-\upsilon^2)}}, \tag{29}$$

where k is the frequency number for the mth order contour-mode. For simplicity, the subscript, m, is omitted for the constants related to the mth order.

With the aid of the free-edged boundary condition, the mth-order contour-mode vibrations of a circular thin-plate resonator can be expressed as [12]

$$u_{r0} = \frac{U_p}{R}\left[kJ_{m-1}(kr') - \frac{m}{r'}J_m(kr') + \frac{m}{r'}\gamma_p J_m(hr')\right]\cos(m\theta) \tag{30a}$$

and

$$u_{\theta 0} = \frac{U_p}{R}\left[\frac{-m}{r'}J_m(kr') - \gamma_p\left(hJ_{m-1}(hr') - \frac{m}{r'}J_m(hr')\right)\right]\sin(m\theta), \tag{30b}$$

where $h = k\sqrt{2/(1-\upsilon)}$, J is the Bessel function of the first kind, γ_p is the contour-mode shape factor, and $r' = r/R$ denotes the dimensionless radial coordinate, which is normalized to the radius of the thin plate. With U_p having the unit of μm^2, U_p/R denotes the vibration amplitude of the mth contour-mode vibrations. Only the modes for which $m \geqslant 2$ are considered here, as these modes have resonant nodes at the edge of a thin plate for locating a support beam [12]. To illustrate the contour-mode vibration behavior, the 2nd, 3rd, and 4th contour-mode shapes are depicted in Fig. 4. The contour-mode vibrations consist of the motion along both the radial and circumferential directions and thus are 2D. The stored maximum vibration energy of the contour-mode vibrations is written as [12]

$$W = \frac{\pi}{2}\rho h\omega^2 U_p^2 \Sigma, \tag{31}$$

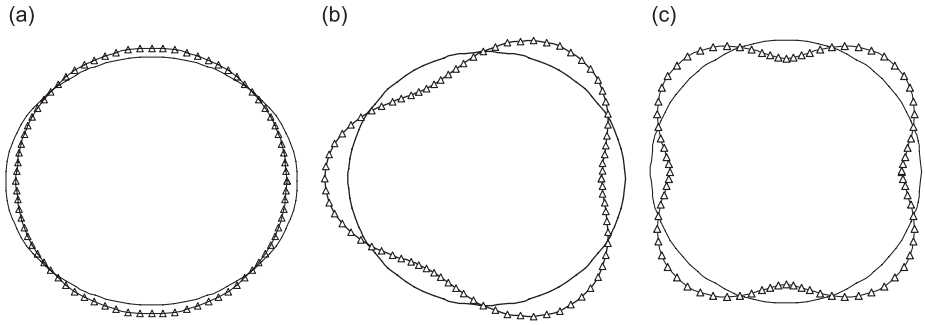

Fig. 4. Contour-mode vibration shapes with triangles symbolizing the vibration modes: (a) $m = 2$, (b) $m = 3$, and (c) $m = 4$.

Table 1
Physical properties of three typical structural materials for micro- and nano-electromechanical resonators

Materials	Silicon $\langle 1\,1\,0 \rangle$ [12]	Silicon $\langle 1\,0\,0 \rangle$ [9]	Polysilicon [25]	Polydiamond [26,27]
Poisson's ratio	0.064	0.28	0.22	0.12
Young's modulus (GPa)	169	130	157	1120
Density (kg/m^3)	2330	2330	2330	3440
Thermal conductivity (W/m K)	90	90	90	1400
Specific heat (J/kg K)	700	700	700	565
Linear thermal expansion coefficient (K^{-1})	2.6×10^{-6}	2.6×10^{-6}	2.6×10^{-6}	1.0×10^{-6}

where

$$\Sigma = \int_0^1 \left(\left[kJ_{m-1}(kr') - \frac{m}{r'} J_m(kr') + \frac{m}{r'} \gamma_p J_m(hr') \right]^2 + \left[\frac{-m}{r'} J_m(kr') - \gamma_p \left(hJ_{m-1}(hr') - \frac{m}{r'} J_m(hr') \right) \right]^2 \right) r' \, \mathrm{d}r'$$

is an integral constant related to the mth contour mode.

While Table 1 lists the mechanical properties of three typical structural materials used in fabrication of MEM and NEM resonators, Table 2 summarizes the constants related to the contour-mode vibrations of circular thin-plate resonators made from these materials. Since the anisotropy of silicon has negligible effect only on the 2nd contour-mode [12], the mechanical properties of single crystal silicon along both the $\langle 1\,1\,0 \rangle$ and $\langle 1\,0\,0 \rangle$ orientations are used only for this mode and are included in Table 2(a).

Consisting of the strain resulting from normal stress and thermal strain arising from the temperature variation, the total normal strains toward the radial, circumferential, and thin-plate thickness directions, take the following forms, respectively:

$$\varepsilon_{rr} = \frac{1}{E}(\sigma_{rr} - \upsilon\sigma_{\theta\theta}) + \alpha_T \Theta, \tag{32a}$$

$$\varepsilon_{\theta\theta} = \frac{1}{E}(\sigma_{\theta\theta} - \upsilon\sigma_{rr}) + \alpha_T \Theta, \tag{32b}$$

$$\varepsilon_{zz} = -\frac{\upsilon}{E}(\sigma_{rr} + \sigma_{\theta\theta}) + \alpha_T \Theta. \tag{32c}$$

Table 2
The related contour-mode constants for a free-edged circular thin-plate resonator

	Silicon ⟨1 0 0⟩	Silicon ⟨1 1 0⟩	Polysilicon	Polydiamond
(a) $m = 2$				
Frequency number (k)	1.4073	1.6002	1.4638	1.5528
Mode shape (γ)	−2.1943	−2.1981	−2.2268	−2.2215
Integral constant for vibration energy (Σ)	1.1651	1.0294	1.1664	1.0939

	Polysilicon	Polydiamond
(b) $m = 3$		
Frequency number (k)	2.2422	2.3703
Mode shape (γ)	−1.1161	−1.1598
Integral constant for vibration energy (Σ)	0.3264	0.3188
(c) $m = 4$		
Frequency number (k)	2.9139	3.0712
Mode shape (γ)	−0.7088	−0.7723
Integral constant for vibration energy (Σ)	0.1379	0.1450

Substituting Eqs. (32a) and (32b) into Eq. (32c) leads to the following expression:

$$\varepsilon_{zz} = -\frac{\upsilon}{(1-\upsilon)}(\varepsilon_{rr} + \varepsilon_{\theta\theta}) + \frac{2\upsilon}{1-\upsilon}\alpha_T\Theta. \tag{32d}$$

According to the contour-mode vibrations, Eqs. (30), the following expression exists for the mth contour mode:

$$\varepsilon_{rr} + \varepsilon_{\theta\theta} = -k^2 J_m(kr')\frac{U_p\cos(m\theta)}{R^2}e^{i\omega t}. \tag{33}$$

Therefore, the elastic dilatation due to the contour-mode vibrations and the temperature variation is written as

$$\nabla\cdot\vec{u} = -\frac{1-2\upsilon}{1-\upsilon}k^2\frac{U_p}{R^2}J_m(kr')\cos(m\theta)e^{i\omega t} + \frac{2\upsilon}{1-\upsilon}\alpha_T\Theta. \tag{34}$$

Owing to its negligible effect, the second term in Eq. (36) will be omitted for the following heat conduction analysis. Fig. 5 illustrates the elastic dilatation amplitude distribution across a circular thin-plate resonator at different contour-mode orders.

5.2. Temperature variation due to the elastic dilatation

With the assumption that the temperature variation is time harmonic, $\Theta = \Theta_0(x)e^{i\omega t}$, and the aid of Eq. (34), the heat conduction equation Eq. (1b) can be rewritten as

$$\nabla^2\Theta_0 + \frac{\omega}{i\chi}\Theta_0 = \frac{\beta_{T2D}T_0\omega}{i\kappa}\left[\frac{1-2\upsilon}{1-\upsilon}k^2\frac{U_p}{R^2}J_m(kr')\cos(m\theta)\right]. \tag{35}$$

The solution to Eq. (35) consists of a general solution, Θ_T, and a particular solution, Θ_s, expressed as below:

$$\Theta_0 = \Theta_T + \Theta_S, \tag{36}$$

where

$$\Theta_T = \Theta_{T0}J_m(k_p r')\cos(m\theta) \tag{37a}$$

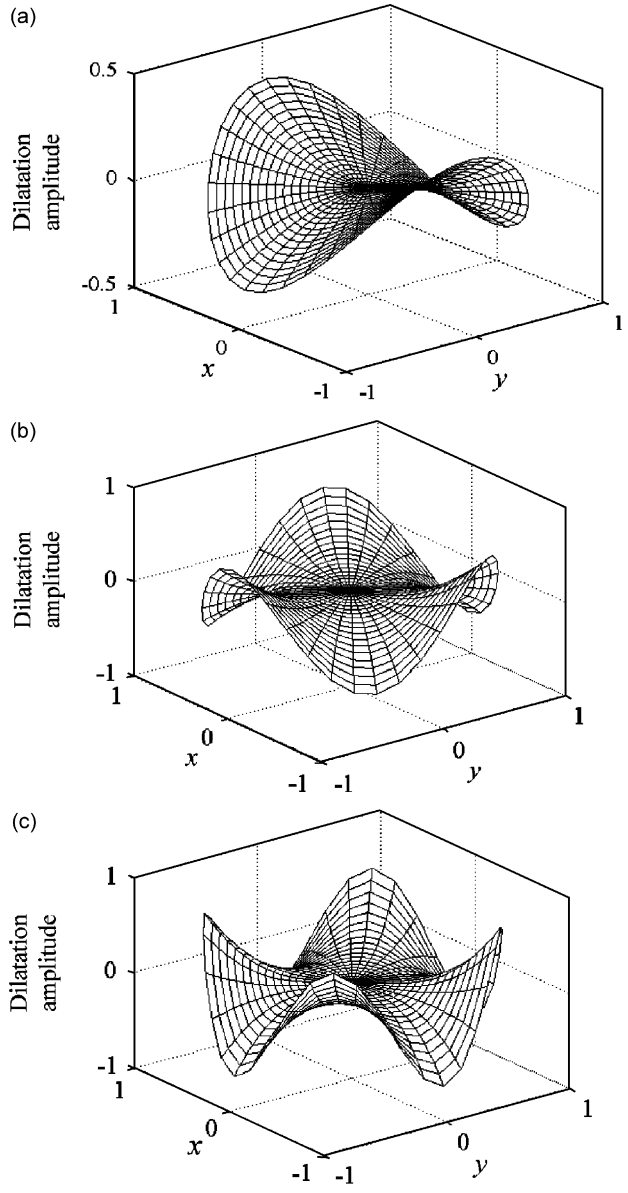

Fig. 5. The elastic dilatation amplitude across a circular thin-plate in the rectangular coordinate (x–y plane) at different contour-modes: (a) $m = 2$, (b) $m = 3$, and (c) $m = 4$. *Note*: Polysilicon is assumed as the structural material; the dilatation amplitude is drawn using the first term of Eq. (34), with $U/R^2 = 1$.

and

$$\Theta_s = \Pi \frac{U_p}{R^2} J_m(kr') \cos(m\theta). \tag{37b}$$

In the above expression, both k_p and Π are complex and are expressed, respectively, as below:

$$k_p = (1 - \mathrm{i})\sqrt{\frac{\omega}{2\chi}} R = (1 - \mathrm{i})\xi_p \quad \text{with} \quad \xi_p = \sqrt{\frac{\omega}{2\chi}} R, \tag{38}$$

$$\Pi = \frac{4\xi_p^4 + 2\xi_p^2 k^2 i}{k^4 + 4\xi_p^4} \cdot \frac{\Delta_E(1-2\upsilon)}{\alpha_T(1-\upsilon)^2} k^2. \tag{39}$$

Based on the adiabatic boundary condition at the edge of the thin plate:

$$\left.\frac{\partial \Theta_T}{\partial r'}\right|_{r'=1} = -\left.\frac{\partial \Theta_s}{\partial r'}\right|_{r'=1}, \tag{40}$$

the amplitude, Θ_{T0}, of the temperature variation in the general solution can be expressed in terms of the mth contour-mode vibration amplitude:

$$\Theta_{T0} = -\Pi \frac{U_p}{R^2} \frac{kJ_{m-1}(k) - mJ_m(k)}{k_p J_{m-1}(k_p) - mJ_m(k_p)}. \tag{41}$$

By substituting Eq. (41) into Eq. (37a), the temperature vibration in the thin plate, Eq. (36), takes the following format:

$$\Theta_0 = -\Pi \frac{U_p}{R^2} \frac{kJ_{m-1}(k) - mJ_m(k)}{k_p J_{m-1}(k_p) - mJ_m(k_p)} J_m(k_p r') \cos(m\theta) + \Pi \frac{U_p}{R^2} J_m(kr') \cos(m\theta). \tag{42}$$

Fig. 6 illustrates the behavior of the imaginary parts of the first term (from the general solution), the second term (from the particular solution) and their total in Eq. (42) versus the radius and the variable, ξ_p, at different contour-mode orders, with $\cos(m\theta) = 1$. It is interesting to note that, in the contour-mode vibrations, the particular solution and the general solution of the temperature variation are both complex and thus contribute to TED. This is different from TED in a flexural-mode beam resonator, in that the particular solution to the temperature variation of a beam resonator is real and does not cause any TED. The complexity of the above expression for the temperature variation makes it unpractical to utilize the complex-frequency approach for calculating TED. In contrast, it will be much easier to calculate TED using the thermal-energy approach, as described in Section 5.3.

5.3. Solution to TED

The substitution of the elastic dilatation, Eq. (34), and the temperature variation, Eq. (42), into Eq. (10) leads to the following expression for the generation of thermal energy in the mth contour-mode vibrations:

$$\Delta Q = \beta_{T2D} \mathrm{i}\pi^2 h \frac{U_p^2}{R^2} k^2 \frac{1-2\upsilon}{1-\upsilon} \Pi \left[\frac{kJ_{m-1}(k) - mJ_m(k)}{k_p J_{m-1}(k_p) - mJ_m(k_p)} \Pi_1 - \Pi_2 \right], \tag{43}$$

where

$$\Pi_1 = \int_0^1 J_m(k_p r') J_m(kr') r' \, \mathrm{d}r' = \frac{1}{k_p^2 - k^2} [kJ_{m-1}(k) J_m(k_p) - k_p \cdot J_{m-1}(k_p) J_m(k)] \tag{44a}$$

and

$$\Pi_2 = \int_0^1 J_m(kr')^2 r' \, \mathrm{d}r' = \frac{1}{2} [J_m(k)^2 - J_{m-1}(k) J_{m+1}(k)]. \tag{44b}$$

Then, the calculated thermal energy, Eq. (43), and the stored maximum vibration energy, Eq. (31), are substituted into the definition of the mechanical quality factor, leading to the expression for the Q_{TED} of the

mth contour-mode vibrations of a circular thin-plate resonator:

$$Q_{\mathrm{TED}}^{-1} = \frac{(1-2\upsilon)^2(1+\upsilon)}{(1-\upsilon)^3}\,\frac{\Delta_E k^2}{\Sigma}\,\mathrm{Re}(\Psi), \tag{45}$$

where

$$\Psi = \frac{4\xi_p^4 \mathrm{i} - 2\xi_p^2 k^2}{k^4 + 4\xi_p^4}\,\frac{kJ_{m-1}(k) - mJ_m(k)}{k_p J_{m-1}(k_p) - mJ_m(k_p)}\,\Pi_1 - \frac{4\xi_p^4 \mathrm{i} - 2\xi_p^2 k^2}{k^4 + 4\xi_p^4}\,\Pi_2. \tag{46}$$

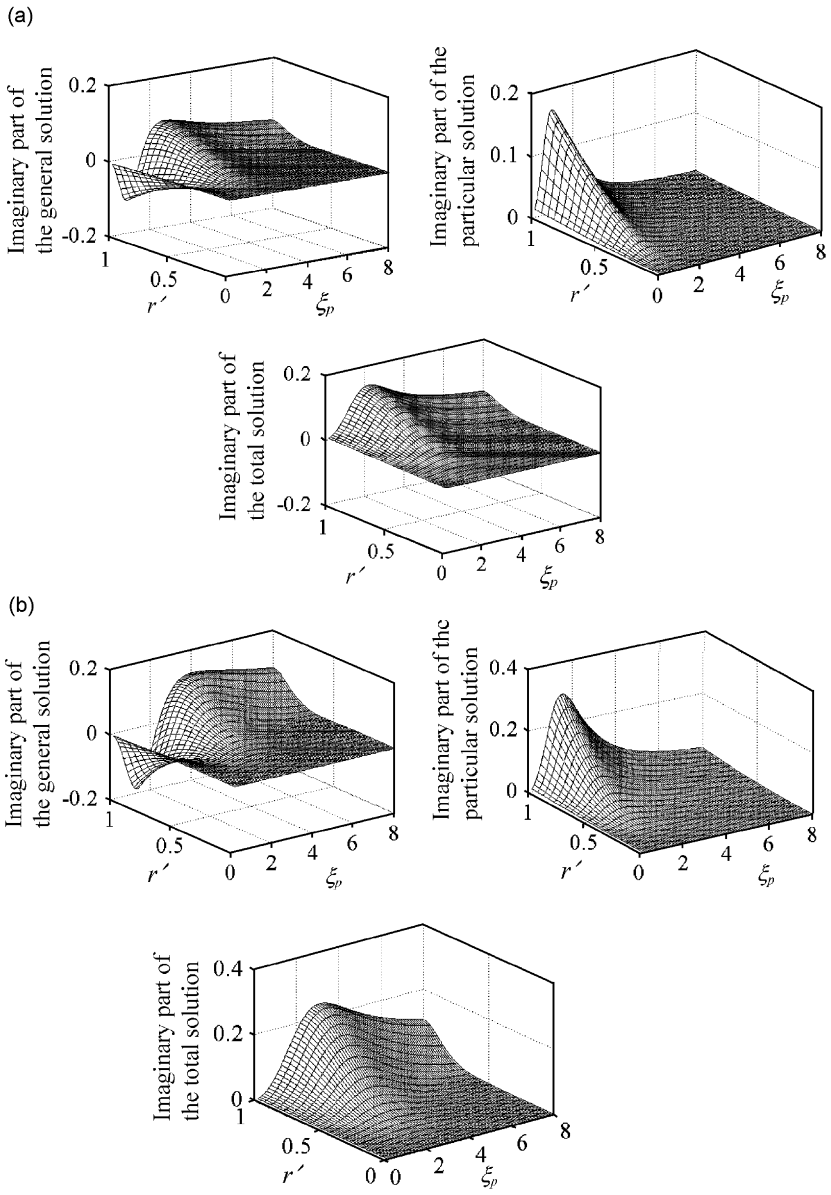

Fig. 6. The behavior of the imaginary parts of the first term, the second term, and their total of the temperature variation in Eq. (42) versus the radius and the variable, ξ_p, at different contour-mode orders (assuming that $U/R^2 = 1/100$, and $\cos(m\theta) = 1$): (a) $m = 2$, (b) $m = 3$, and (c) $m = 4$. *Note*: Polysilicon is assumed as the structural material.

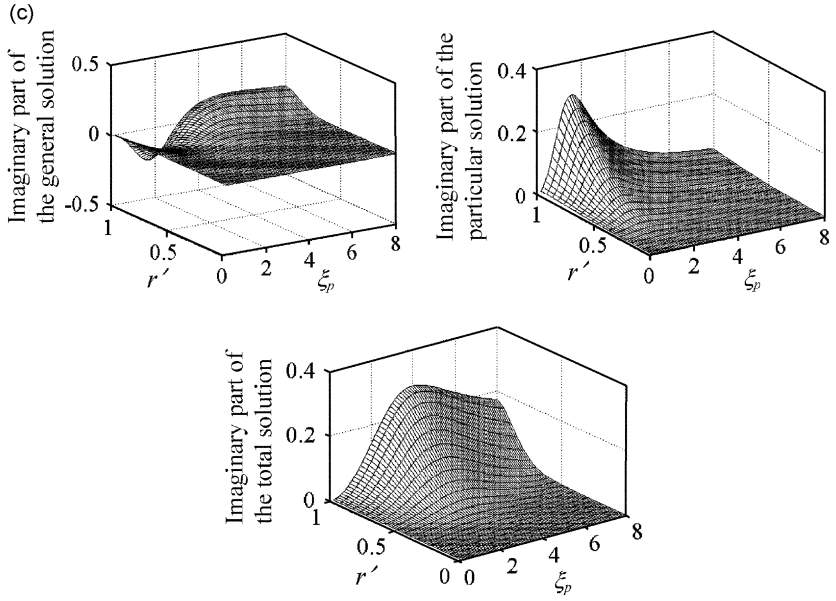

Fig. 6. (*Continued*)

Fig. 7 illustrates the behavior of the real parts from the first term (corresponding to the general solution), the second term (corresponding to the particular solution), and their total in Eq. (46) versus the variable, ξ_p. From this figure, it is found that the value for $\xi_{p\max}$, at which maximum TED occurs, varies with the contour-mode orders. This is different from TED in a flexural-mode beam resonator, where maximum TED occurs at the value of $\xi_{b\max} \cong 2.225$, regardless of its flexural-mode orders [9].

6. Discussion

In practice, the main concern of TED is its dependence on the radius and resonant frequency of a circular thin-plate resonator. Therefore, Figs. 8 and 9 illustrate the behavior of thermeoalstic damping versus the variable, ξ_p, thin-plate radius, and resonant frequency of circular thin-plate resonators made from polysilicon and polydiamond, respectively. It becomes clear that both the Q_{TED} value of a thin-plate resonator of the same radius and the minimum Q_{TED} decrease with the increasing contour-mode orders. From these figures, it is further found that the minimum Q_{TED} of the contour-mode vibrations occurs at the resonant frequency as high as a few tens of gigahertz, or alternately at the radius of 40–400 nm. This indicates that TED becomes a significant source of dissipation for circular thin-plate resonators at the nanometer scale. For a circular thin-plate resonator with a resonant frequency below 1 GHz, its Q_{TED} is well above 1×10^6. Table 3 summarizes the minimum values of Q_{TED} and their corresponding frequencies and radii for the structural materials listed in Table 1.

This paragraph addresses the difference in TED between the flexural-mode vibrations of a beam resonator and the contour-mode vibrations of a circular thin-plate resonator. For a flexural-mode beam resonator, the particular solution to the temperature variation, the last term on the right-hand side of Eq. (19), is a linear function of the variable, y. Therefore, based on Eq. (5), the entropy change ($\partial^2\Theta_0/\partial y^2$) caused by the particular solution is zero. For this reason, the particular solution to the temperature variation does not contribute to TED. This may explain the observation that the value of $\xi_{b\max}$ does not vary with the flexural-mode orders of a beam resonator. On the contrary, for a circular thin-plate resonator, the particular solution to the temperature variation, the second term on the right-hand side of Eq. (42), is a complicate function of the variables of r' and θ, and at the same time, has a complex amplitude (due to the time-harmonic assumption of heat conduction). Hence, the entropy change ($\nabla^2\Theta_0$) caused by the particular solution is non-zero, indicating

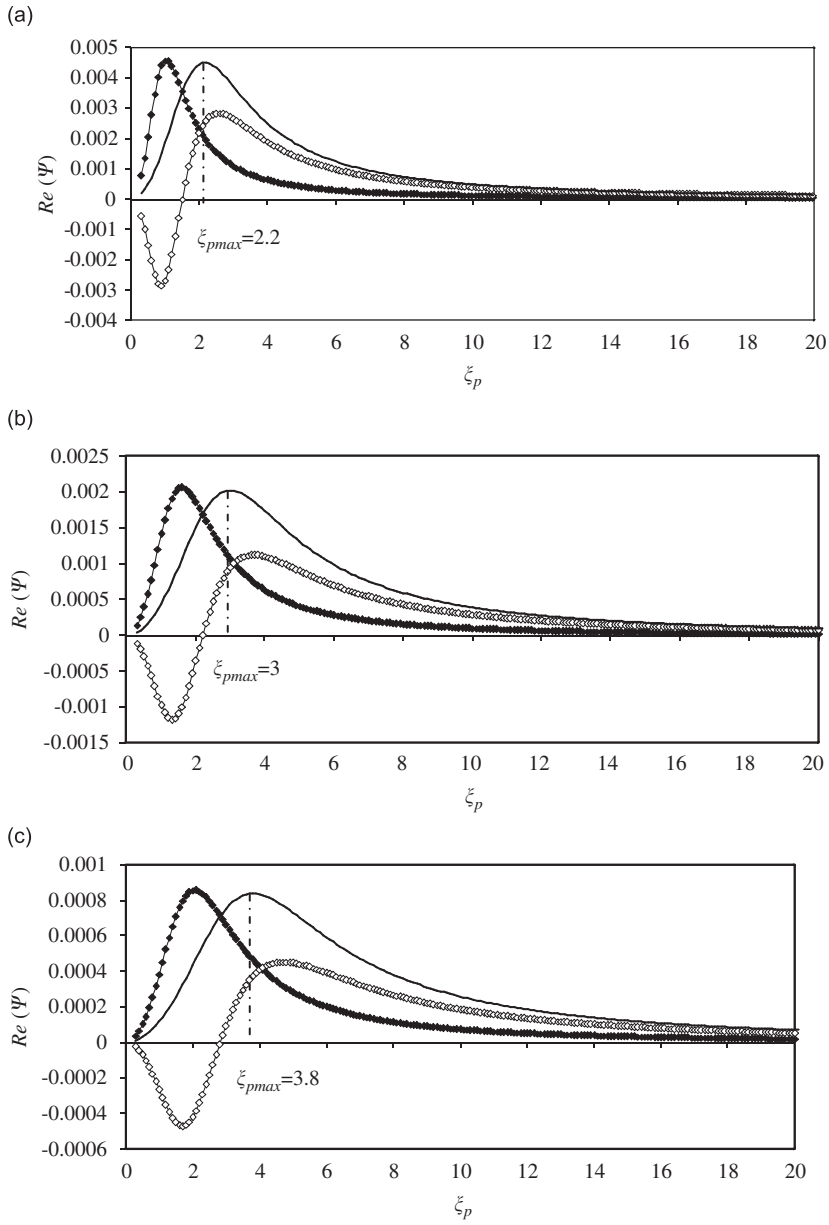

Fig. 7. The behavior of the real parts of the first term, the second term, and their total in Eq. (46) versus the variable, ξ_p, at different contour-mode orders: (a) $m = 2$, (b) $m = 3$, and (c) $m = 4$. *Note*: Polysilicon is assumed as the structural material. —◆— Particular, —◇— general, —— total.

that the particular solution to the temperature variation is not completely in phase with the elastic dilatation and contributes to TED. Moreover, as illustrated in Figs. 7–9, the contribution of the particular solution to TED manifests itself by varying the value of $\xi_{p\max}$ and maximum TED with the contour-mode orders, because the particular solution to the temperature variation corresponds to the elastic dilatation at different contour-mode orders. At last, it is worth mentioning that maximum TED occurs at extremely high frequencies of the contour-mode vibrations of a circular thin-plate resonator, as compared with its counterpart in a flexural-mode beam resonator.

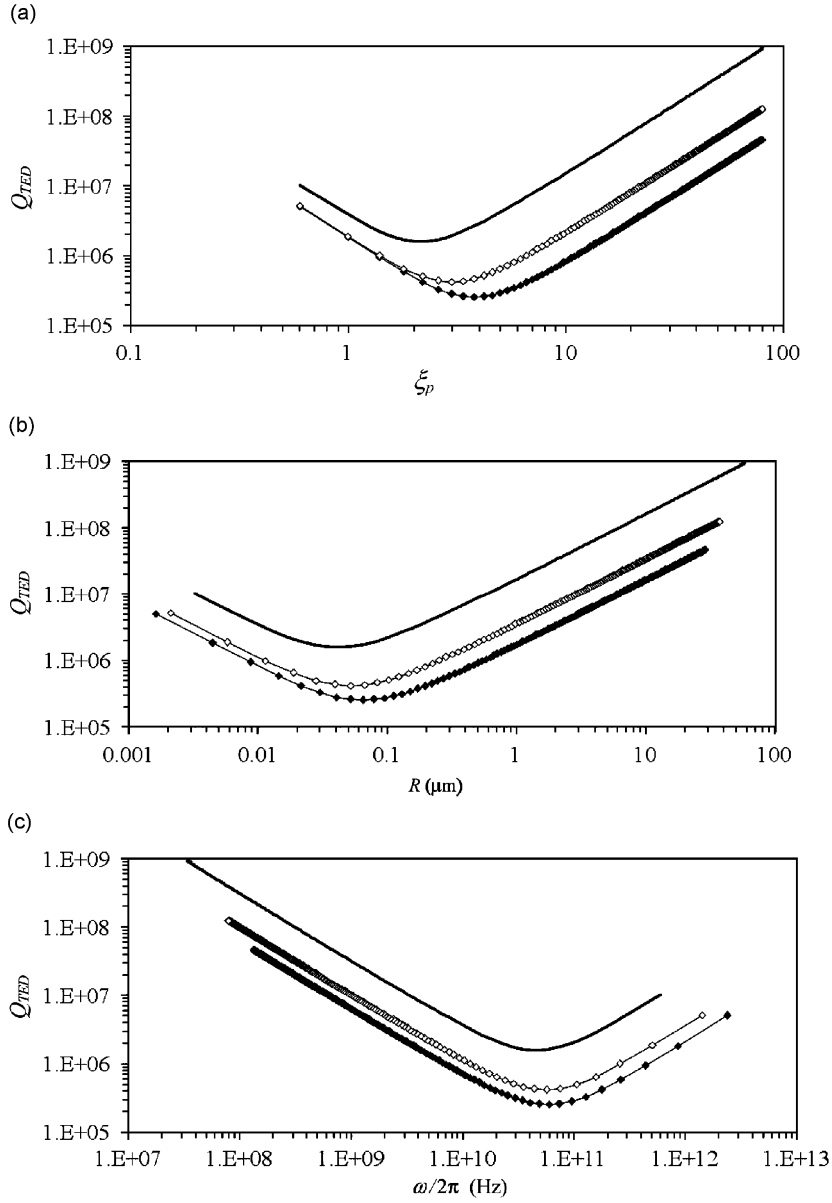

Fig. 8. The behavior of the Q_{TED} of a *polysilicon* thin-plate resonator versus (a) the variable, ξ_p, (b) thin-plate radius, R, and (c) the resonant frequency, $\omega/2\pi$. —◆— $m = 4$, —◇— $m = 3$, —— $m = 2$.

7. Conclusion

In this paper, a thermal-energy approach for calculating TED has been presented and verified by the well-known solution to TED in a flexural-mode beam resonator. By using this approach, TED in the contour-mode vibrations of a free-edged circular thin-plate resonator is predicted. The dependence of the Q_{TED} on the thin-plate radius, resonant frequency, and contour-mode orders is investigated. This work has established that the Q_{TED} of a circular thin-plate resonator is well above 1×10^6 when its resonant frequency is below 1 GHz; and TED becomes a significant source of dissipation for circular thin-plate resonators at the nanometer scale.

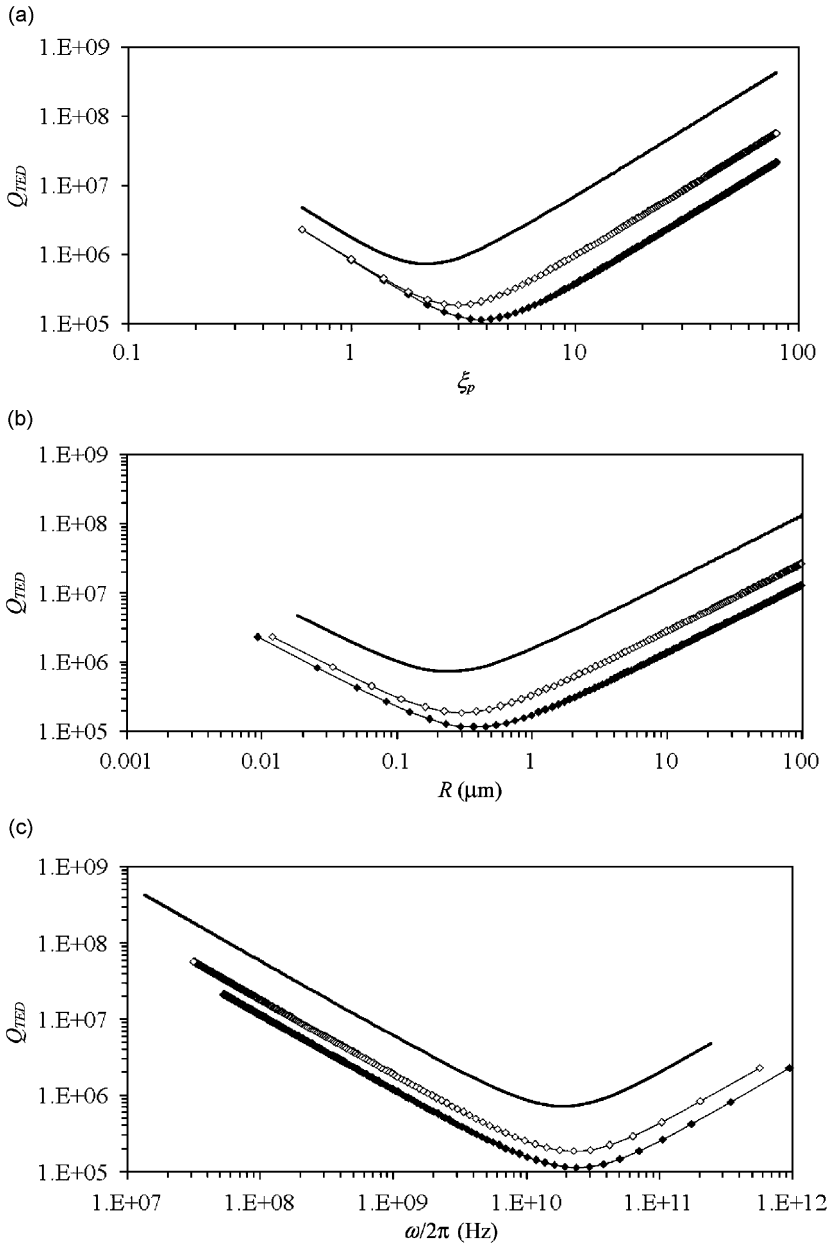

Fig. 9. The behavior of the Q_{TED} of a *polydiamond* thin-plate resonator versus (a) the variable, ξ_p, (b) thin-plate radius, R, and (c) the resonant frequency, $\omega/2\pi$. —♦— $m = 4$, —◇— $m = 3$, —— $m = 2$.

Throughout this paper, the continuum theory of elasticity is assumed to analyze the behavior of thin-plate resonators at the nanoscale, where atomic-level in-homogeneities come to the fore. It has been demonstrated [28] that the traditional continuum theory breaks down at the nanometer scale and, however, the elasticity of nanoscale structures might be modified by atomic-level elasticity, in terms of physical observables, correctly summed to give exact overall elastic response. Accordingly, either the results of our analysis might be still valid but need modified elasticity at nanoscale, or a completely new theory at atomic-level might be required to describe TED in circular thin-plate resonators at the nanometer scale.

Table 3
The minimum values of Q_{TED} and their corresponding frequencies and radii for the contour-mode vibrations in circular thin-plate resonators

	Silicon ⟨1 0 0⟩	Silicon ⟨1 1 0⟩	Polysilicon	Polydiamond
Δ_E	1.616×10^{-4}	2.101×10^{-4}	1.952×10^{-4}	1.729×10^{-4}
$m = 2$ ($\xi_{p\max} = 2.2$)				
Minimum Q_{TED}	3.668×10^{6}	3.880×10^{5}	1.605×10^{6}	7.358×10^{5}
Frequency (GHz)	35.7	55.6	45.2	18.2
Radius (nm)	48	39	43	247
$m = 3$ ($\xi_{p\max} = 3.0$)				
Minimum Q_{TED}			4.240×10^{5}	1.900×10^{5}
Frequency (GHz)			57.0	22.8
Radius (nm)			53	301
$m = 4$ ($\xi_{p\max} = 3.8$)				
Minimum Q_{TED}			2.574×10^{5}	1.168×10^{5}
Frequency (GHz)			60.1	23.8
Radius (nm)			65	373

References

[1] G. Stemme, Resonant silicon sensors, *Journal of Micromechanics and Microengineering* 1 (1991) 113–125.
[2] H.A.C. Tilmans, M. Elwebspoek, J.H.J. Fluitman, Micro resonant force gauges, *Sensors and Actuators A* 30 (1992) 35–53.
[3] N. Yazdi, F. Ayazi, K. Najafi, Micromachined inertial sensors, *Proceedings of the IEEE* 86 (8) (1998) 1640–1659.
[4] K. Wang, A.-C. Wong, C.T.-C Nguyen, VHF free–free beam high-Q micromechanical resonators, *Journal of Microelectromechanical Systems* 9 (3) (2000) 347–360.
[5] S. Pourkamali, F. Ayazi, Electrically coupled MEMS bandpass filters—part I: with coupling element, *Sensors and Actuators A* 122 (2005) 307–316.
[6] S. Pourkamali, F. Ayazi, Electrically coupled MEMS bandpass filters—part II: without coupling element, *Sensors and Actuators A* 122 (2005) 317–325.
[7] C.T.-C. Nguyen, Frequency-selective MEMS for miniaturized communication devices, *Proceedings of the IEEE Aerospace Conference*, Vol. 1, 1998, pp. 445–460.
[8] Z. Hao, A. Erbil, F. Ayazi, An analytical model for support loss in micromachined beam resonators with in-plane flexural vibrations, *Sensors and Actuators A* 109 (2003) 156–164.
[9] R. Lifshitz, M.L. Roukes, Thermoelastic damping in micro- and nanomechanical systems, *Physical Review B* 61 (8) (2000) 5600–5609.
[10] K.Y. Yasutnura, T.D. Stowe, E.M. Chow, T. Pfafman, T.W. Kenny, B.C. Stipe, D. Rugar, Quality factors in micron- and submicron-thick cantilevers, *Journal of Microelectromechanical Systems* 9 (1) (2000) 117–125.
[11] J. Yang, T. Takahito Ono, Masayoshi Esashi, Energy dissipation in submicrometer thick single-crystal silicon cantilevers, *Journal of Microelectroemchanical Systems* 11 (9) (2002) 775–783.
[12] Z. Hao, S. Pourkamali, F. Ayazi, VHF single crystal silicon elliptic bulk-mode capacitive disk resonators—part I: design and modeling, *Journal of Microelectromechanical Systems* 13 (6) (2004) 1043–1053.
[13] S. Pourkamali, Z. Hao, F. Ayazi, VHF single crystal silicon elliptic bulk-mode capacitive disk resonators—part II: implementation and characterization, *Journal of Microelectromechanical Systems* 13 (6) (2004) 1054–1062.
[14] M.A. Abdelmoneum, M.U. Demirci, C.T.-C. Nguyen, Steamless wine-glass-mode disk micromechanical resonators, *Proceeding of the IEEE International Micro Electro Mechanical Systems Conference (MEMS'03)*, January 2003, pp. 698–701.
[15] Z. Hao, F. Ayazi, Supportloss in micromechanical disk resonators, *Proceedings of the IEEE Micro Electro Mechanical Systems Conference (MEMS'05)*, January 2005, pp. 137–141.
[16] W. Nowacki, *Dynamic Problems of Thermoelasticity*, Noordhoff, Leyden, 1975.
[17] I.N. Sneddon, R. Hill, *Progress in Solid Mechanics*, Vol. I, North-Holland, Amsterdam, 1960.
[18] C. Zener, Internal friction in solids, I. Theory of internal friction in reeds, *Physical Review* 52 (1937) 230–235.
[19] C. Zener, Internal friction in solids, II. General theory of thermoelastic internal friction, *Physical Review* 53 (1938) 90–99.
[20] Z. Hao, F. Ayazi, Thermoelastic damping in flexural-mode ring gyroscopes, *2005 ASME International Mechanical Engineering Congress and Exposition (IMECE 2005)*, November 2005 IMECE2005-79965.
[21] S.J. wong, C.H.J. Fox, S. McWilliam, Thermoelastic damping of the in-plane vibration of thin silicon rings, *Journal of Sound and Vibration* 293 (2006) 266–285.

[22] L. Malinowskim, Relaxation model for heat conduction and generation and the second law, *Journal of Physics D: Applied Physics* 27 (1994) 2031–2034.
[23] R.A. Johnson, *Mechanical Filters in Electronics*, Wiley, New York, 1983.
[24] J.N. Reddy, *An Introduction to the Finite Element Method*, McGraw-Hill, New York, 2006.
[25] A. Duwel, R.N. Candler, T.W. Kenney, M. Varghese, Engineering MEMS resonators with low thermoelastic damping, *Journal of Microelectromechanical Systems* 15 (6) (2006) 1437–1445.
[26] J. Philip, P. Hess, T. Feygelson, J.E. Butler, S. Chattopadhyay, K.H. Chen, L.C. Chen, Elastic, mechanical, and thermal properties of nanocrystalline diamond films, *Journal of Applied Physics* 93 (4) (2003) 2164–2171.
[27] T. Sato, K. Ohashi, T. Sudoh, K. Haruna, H. Maeta, Thermal expansion of a high purity synthetic diamond single crystal at low temperature, *Physical Review B* 65 (2002) 092102 (R).
[28] D.E. Segall, Sohrab Ismail-Beigi, T.A. Arias, *Physical Review B* 65 (2002) 214109.